Thin Films

DOI: 10.1002/anie.200602670

Synthesis and Structure of Ultrathin Aluminosilicate Films**

Dario Stacchiola, Sarp Kaya, Jonas Weissenrieder, Helmut Kuhlenbeck, Shamil Shaikhutdinov, Hans-Joachim Freund, Marek Sierka, Tanya Kumanova Todorova, and Joachim Sauer*

Inorganic-chemistry textbooks define aluminosilicates as silicates in which some of the Si^{4+} ions are replaced by Al^{3+} ions. The excess negative charge arising from the replacement is balanced by positive ions, such as H^+ or alkali-metal cations. Zeolites are important microporous members of the aluminosilicate family, which have a large variety of applications ranging from catalysis and adsorption to agriculture and construction.[1] Both experimental and theoretical studies of zeolites, in particular, the precise determination of the catalytically active sites, are often hampered by the structural and chemical complexity of these compounds.[2] The employment of surface-sensitive techniques to elucidate the mechanism of catalytic reactions on zeolites at a fundamental level is challenging. Owing to the insulating properties of aluminum–silicon oxides, this approach can only be successful when applied to thin films grown on conducting metal substrates, as demonstrated for many binary oxides (for example, alumina, silica, magnesia, or iron oxides).[3–6] Thin zeolite films are also currently used in membrane technology,[7] chemical sensors,[8] and optoelectronic devices.[9]

Herein, we report the preparation of ordered ultrathin aluminosilicate films on a metal substrate. The atomic structure of the films was determined using scanning tunneling microscopy (STM), infrared reflection absorption spectroscopy (IRAS), photoelectron spectroscopy (PES) with synchrotron radiation, and density functional theory (DFT) calculations. This approach can be further developed for the preparation of thin zeolite films as model systems for atomistic studies of zeolite surfaces.

We have recently shown that an ordered thin silica film consisting of a two-dimensional (2D) network of corner-sharing $\{SiO_4\}$ tetrahedra can be grown on a Mo(112) substrate.[10–13] One oxygen atom of each $\{SiO_4\}$ tetrahedron in the film points towards molybdenum atoms in the substrate. Deposition of aluminum onto the film and subsequent annealing in vacuum leads to a partial reduction of the silica, as evidenced by X-ray photoelectron spectroscopy (XPS). This sequential preparation destroys the long-range order in the original silica film, as shown by low-energy electron diffraction (LEED). STM inspection of the product revealed a rough surface with particle-like features, which were interpreted as alumina nanoparticles embedded in the silica film. This observation is consistent with the results of Gründling et al., who obtained disordered Al_2O_3–SiO_2 films by vacuum annealing samples consisting of aluminum deposited onto approximately 3-nm-thick silica films on Mo(100) substrates.[14]

To facilitate the intermixing of aluminum and silicon in the film, we codeposited aluminum and silicon onto an O/Mo(112) surface in an oxygen environment (see Experimental Section). In the subsequent annealing in vacuum, the temperature was increased in steps, until LEED analysis of the film indicated an ordered structure.

After annealing films with low Al/Si ratios (less than 0.2) at 1100 K, a sharp LEED pattern corresponding to a c(2×2) structure on the Mo(112) surface, similar to that of the pure silica film, was observed. XPS investigation of these films indicated that the silicon and aluminum atoms are in fully oxidized states.

STM images of the mixed-oxide films reveal atomically flat terraces with only a few nanoparticles at their edges (Figure 1a). High-resolution images show the same honeycomb structure and antiphase domain boundaries reported

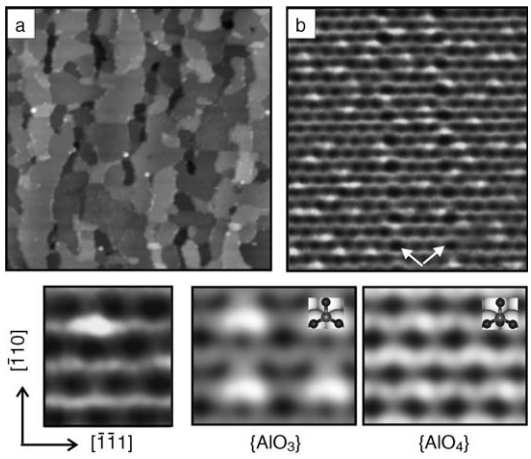

Figure 1. Top: STM images of an aluminosilicate film (Al/Si ≈ 1:5) on a Mo(112) substrate. Sizes and tunneling parameters: a) 100×100 nm^2, $V_s = 1.6$ V, $I = 0.2$ nA; b) 8×6 nm^2, $V_s = 1.2$ V, $I = 0.3$ nA. The arrows in (b) indicate antiphase domain boundaries along the molybdenum [$\bar{1}$10] direction. Bottom: simulated STM images for the $\{AlO_3\}$ and $\{AlO_4\}$ models are compared with an enlarged section of image (b). The $\{AlO_3\}$ and $\{AlO_4\}$ units are superimposed on the simulated images.

[*] Dr. D. Stacchiola, S. Kaya, Dr. J. Weissenrieder, Dr. H. Kuhlenbeck, Dr. S. Shaikhutdinov, Prof. H.-J. Freund
Department of Chemical Physics
Fritz-Haber-Institut der Max-Planck-Gesellschaft
Faradayweg 4–6, Berlin 14195 (Germany)
Fax: (+49) 30-84134105
E-mail: shaikhutdinov@fhi-berlin.mpg.de
Homepage: http://www.fhi-berlin.mpg.de/cp
Dr. M. Sierka, T. K. Todorova, Prof. J. Sauer
Humboldt-Universität zu Berlin
Institut für Chemie
Unter den Linden 6, Berlin 10099 (Germany)

[**] We acknowledge financial support from the Fonds der Chemischen Industrie and the EU Project GSOMEN. D.S. and J.W. thank the Alexander von Humboldt Foundation for fellowships. T.K.T. and S.K. acknowledge the International Max Planck Research School "Complex Surfaces in Materials Science". We also thank the Norddeutscher Verbund für Hoch- und Höchstleistungsrechnen (HLRN) for computing time.

WILEY InterScience DISCOVER SOMETHING GREAT
© 2006 Wiley-VCH Verlag GmbH & Co. KGaA, Weinheim

for the silica films (Figure 1b).[11,12] However, in contrast to the pure silica films, numerous bright spots were detected on the surface of the aluminosilcate films. These spots are approximately 0.2 Å higher than the neighboring protrusions. The density of the spots correlates well with the aluminum coverage determined by XPS, and their random distribution indicates a random distribution of the aluminum atoms in the film. The protrusions are slightly elongated along one of the principal directions of the silica lattice, which coincides with the $[\bar{1}\bar{1}1]$ direction of the Mo(112) surface (additional experiments demonstrated that this is not a tip artifact).

On the basis of these LEED and STM results, we propose that the structure of the aluminosilicate film consists of a 2D network of corner-sharing $\{SiO_4\}$ tetrahedra, in which some Si^{4+} ions are replaced by Al^{3+} ions. The charge defects introduced by the Al^{3+} ions must be compensated. In bulk aluminosilicates, this compensation is achieved by the intercalation of H^+ or alkali-metal cations. Alkali metals were not present during the film preparation, and H^+ ions were not detected by vibrational or electron spectroscopy. However, the extra charge in thin films can be easily accommodated by the electron reservoir of the metal substrate. In this $\{AlO_4\}$ model, the Al^{3+} ions are each coordinated to four O^{2-} ions in the same geometry as the Si^{4+} ions in the pure silica film (Figure 2). Another possibility is that the Al^{3+} ions are coordinated by three O^{2-} ions from the top layer of the film, but are not bonded to an O^{2-} ion at the substrate interface ($\{AlO_3\}$ model; Figure 2).

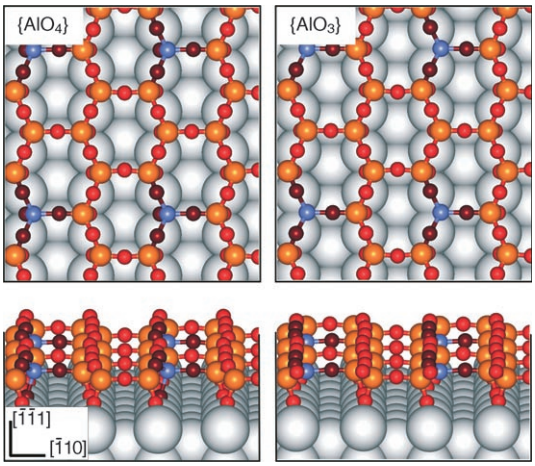

Figure 2. Top and side views of the $\{AlO_4\}$ and $\{AlO_3\}$ models of aluminosilicate films on a Mo(112) substrate. Mo gray, Al blue, Si orange, O red.

These two models were examined with DFT calculations by considering a (4×2) surface cell, in which one of the eight silicon atoms was replaced by an aluminum atom, resulting in compositions of $AlSi_7O_{20}$ for the $\{AlO_4\}$ model and $AlSi_7O_{19}$ for the $\{AlO_3\}$ model. Both models are minima on the potential energy surface.[15]

For the STM image shown in Figure 1b, the tunneling parameters were chosen such that the oxygen atoms in the topmost layer of the film are detected as protrusions.[11,12] In the images simulated from the DFT-optimized structures of the $\{AlO_4\}$ and $\{AlO_3\}$ models, the aluminum-bonded surface oxygen atoms, which have a higher corrugation amplitude, are brighter than the silicon-bonded oxygen atoms (Figure 1). This effect is more pronounced for the $\{AlO_3\}$ model, because of the enhanced relaxation associated with the absence of aluminum-bonded interface oxygen atoms. Comparison of the experimental and simulated STM images, therefore, favors the $\{AlO_3\}$ model.

Further support for the $\{AlO_3\}$ model comes from high-resolution PES. In PE spectra of the silica films (Figure 3, top spectra), the O 1s region, which is much better resolved than

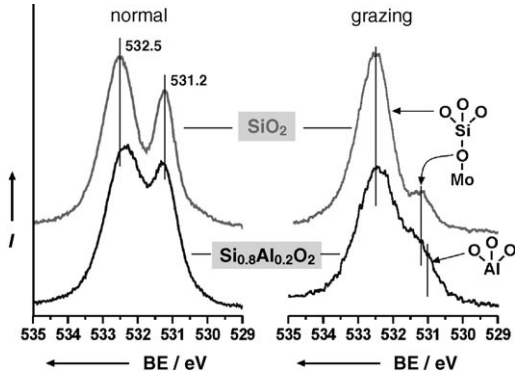

Figure 3. O 1s region of the PE spectra of silica (top) and aluminosilicate (bottom: Al/Si ≈ 1:5) films recorded at normal and grazing emission angles.

by conventional XPS,[11–13] comprises two distinct peaks, which are assigned to oxygen species in the top layer (at 532.5 eV) and in the molybdenum-bonded interface layer (at 531.2 eV).[11] The signal at lower binding energy (BE) is strongly attenuated when the spectrum is measured at a grazing emission angle, confirming that the associated oxygen species are located in the subsurface region. The presence of interface oxygen atoms is also manifested by a well-resolved signal at 228.2 eV in the Mo 3d region (not shown), which is attributed to partially oxidized molybdenum atoms at the substrate surface (a signal at 228.0 eV is also observed, which is assigned to metallic molybdenum).

As a result of the presence of approximately 20 mol% aluminum in the aluminosilicate film, the O 1s signals in the PE spectra broaden (see Figure 3, bottom spectra), because the oxygen atoms (which are bonded to silicon and/or aluminum atoms) occupy a variety of environments. Our DFT calculations revealed that the oxygen atoms in Si-O-Al units have a BE of 531 eV, which overlaps with that of the interface oxygen atoms in Si-O-Mo units. As a result, the intensity of the lower-BE O 1s signal is notably higher in the PE spectrum of the aluminosilicate film than in that of the pure silica film. Because the aluminum-bonded oxygen atoms are in the top layer of the film, this signal is less attenuated in the aluminosilicate spectrum recorded at a grazing emission angle. According to our calculations, the oxygen atoms in the

 © 2006 Wiley-VCH Verlag GmbH & Co. KGaA, Weinheim

Al-O-Mo units of the $\{AlO_4\}$ model should be manifested by a signal at 530 eV, which is not observed experimentally. Therefore, our PES results also favor the $\{AlO_3\}$ model.

The IR spectra of the silica and aluminosilicate films, as well as the calculated frequencies for the $\{AlO_3\}$ model are presented in Figure 4. Note that only vibrations resulting in

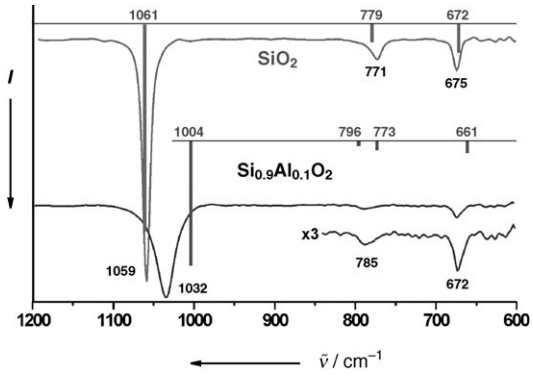

Figure 4. IR spectra of silica and aluminosilicate (Al/Si ≈ 1:9) films. An enlargement of the low-frequency region of the aluminosilicate spectrum is also shown. Bars indicate the frequencies calculated for the $\{AlO_3\}$ model; the height of the bars is proportional to the signal intensity.

changes in the dipole moment that are perpendicular to the surface can be detected, owing to the presence of the metal substrate. The main peak at 1059 cm^{-1} in the spectrum of the silica film appears as a significantly broadened peak at 1032 cm^{-1} in the spectrum of the aluminosilicate film. This signal originates from asymmetric Si-O-Mo stretching vibrations[11,12] and is, therefore, strongly influenced by the partial replacement of silicon by aluminum. The line broadening in the aluminosilicate spectrum is consistent with the less-ordered structure of the film relative to that of the pure silica film. The weak IR features at 771 and 675 cm^{-1} in the silica spectrum, which are assigned to symmetric stretching and bending modes, are also altered in the aluminosilicate spectrum.

The agreement between the calculated and experimental frequencies is not as good as for the silica films. This discrepancy can be partially explained by the relatively small (4×2) unit cell used in the calculations, which results in an ordered superstructure, whereas in the real film the aluminum atoms are randomly dispersed. Nonetheless, the calculations correctly predict the direction of the energy shift of the main signal, as well as the splitting of the signal near 770 cm^{-1}.

In summary, the preparation of an ordered aluminosilicate film on a metal substrate has been achieved through the codeposition of aluminum and silicon onto a Mo(112) surface in an O_2 atmosphere and subsequent vacuum annealing. Experimental and theoretical results show that, in aluminosilicate films with low Al/Si ratios, aluminum atoms partially replace the silicon atoms of the silica structure to form a 2D network of corner-sharing $\{AlO_3\}$ and $\{SiO_4\}$ units.

Experimental Section

The experiments were carried out in an ultra-high vacuum (UHV) chamber (base pressure 2×10^{-10} mbar) equiped with LEED, XPS, IRAS, and STM. The aluminosilicate films were prepared by a method similar to that described for the preparation of silica films.[11,12] Aluminum and silicon were codeposited onto a p(2×3)-O-Mo(112) surface at 900 K in an O_2 atmosphere (5×10^{-8} mbar). The total amounts of aluminum and silicon at different Al/Si ratios corresponded to slightly more than one monolayer (relative to the Mo(112) substrate). The mixed-oxide overlayer was then annealed at 1100 K in vacuum for 5 min. The PES experiments using synchrotron radiation were performed in a UHV chamber at BESSY II (beamline UE52-PGM1) with a Scienta R4000 analyzer (energy resolution below 200 meV).

The methodology applied in the DFT calculations was described previously.[11–13] The Vienna ab initio simulation package (VASP)[16,17] was used with the Perdew–Wang (PW91) exchange-correlation functional[18] and the projector augmented wave (PAW) method.[19,20] The basis set consisted of plane waves with energies up to 400 eV, and a $4\times4\times1$ Monkhorst–Pack grid was used for the generation of k points.[21] The vibrational spectra were calculated using the central finite-difference method; intensities were determined from the derivative of the dipole-moment component perpendicular to the surface. To compensate for systematic errors of DFT, we applied an empirical scaling factor of 1.0312 to the calculated frequencies.[11,22] Core-level binding energies including final state effects were calculated using a modified PAW method. STM images were simulated from the self-consistent charge density by employing the Tersoff–Hamann approach.[23]

Received: July 5, 2006
Revised: August 17, 2006
Published online: October 19, 2006

Keywords: aluminosilicates · mixed oxides · thin films · zeolites

[1] *Introduction to Zeolite Science and Practice* (*Studies in Surface Science and Catalysis*, *Vol. 137*), (Eds.: H. van Bekkum, P. A. Jacobs, E. M. Flanigen, J. C. Jansen), Elsevier, Amsterdam, **2001**.
[2] M. Sierka, J. Sauer, *J. Phys. Chem. B* **2001**, *105*, 1603.
[3] M. Bäumer, H.-J. Freund, *Prog. Surf. Sci.* **1999**, *61*, 127.
[4] S. Chambers, *Surf. Sci. Rep.* **2000**, *39*, 105.
[5] S. Wendt, Y. D. Kim, D. W. Goodman, *Progr. Surf. Sci.* **2003**, *74*, 141.
[6] W. Weiss, W. Ranke, *Progr. Surf. Sci.* **2002**, *70*, 1.
[7] J. Choi, S. Ghosh, Z. Lai, M. Tsapatsis, *Angew. Chem.* **2006**, *118*, 1172; *Angew. Chem. Int. Ed.* **2006**, *45*, 1154.
[8] J. Coronas, J. Santamaria, *Top. Catal.* **2004**, *29*, 29.
[9] G. Shu, J. Liu, A. S. T. Chiang, R. W. Thompson, *Adv. Mater.* **2006**, *18*, 185.
[10] T. Schroeder, M. Adelt, B. Richter, M. Naschitzki, J. B. Giorgi, M. Bäumer, H.-J. Freund, *Surf. Rev. Lett.* **2000**, *7*, 7.
[11] J. Weissenrieder, S. Kaya, J. L. Lu, H. J. Gao, S. Shaikhutdinov, H. J. Freund, M. Sierka, T. K. Todorova, J. Sauer, *Phys. Rev. Lett.* **2005**, *95*, 076103.
[12] T. K. Todorova, M. Sierka, J. Sauer, S. Kaya, J. Weissenrieder, J.-L. Lu, H.-J. Gao, S. Shaikhutdinov, H.-J. Freund, *Phys. Rev. B* **2006**, *73*, 165414.
[13] M. Sierka, T. K. Todorova, S. Kaya, D. Stacchiola, J. Weissenrieder, J.-L. Lu, H.-J. Gao, S. Shaikhutdinov, H.-J. Freund, J. Sauer, *Chem. Phys. Lett.* **2006**, *424*, 115.
[14] Ch. Gründling, J. A. Lercher, D. W. Goodman, *Surf. Sci.* **1994**, *318*, 97.
[15] Because of the different chemical compositions of the models, their relative stabilities may depend on the oxygen partial

 © 2006 Wiley-VCH Verlag GmbH & Co. KGaA, Weinheim

pressure. A full DFT analysis will be presented in future publications.
[16] G. Kresse, J. Furthmüller, *Comput. Mater. Sci.* **1996**, *6*, 15.
[17] G. Kresse, J. Furthmüller, *Phys. Rev.* B **1996**, *54*, 11169.
[18] J. P. Perdew, J. A. Chevary, S. H. Vosko, K. A. Jackson, M. R. Pederson, D. J. Singh, C. Fiolhais, *Phys. Rev. B* **1992**, *46*, 6671.
[19] P. E. Blöchl, *Phys. Rev. B* **1994**, *50*, 17953.
[20] G. Kresse, D. Joubert, *Phys. Rev. B* **1999**, *59*, 1758.
[21] H. J. Monkhorst, J. D. Pack, *Phys. Rev. B* **1976**, *13*, 5188.
[22] A. P. Scott, L. Radom, *J. Phys. Chem.* **1996**, *100*, 16502.
[23] J. Tersoff, D. R. Hamann, *Phys. Rev. B* **1985**, *31*, 805.

 © 2006 Wiley-VCH Verlag GmbH & Co. KGaA, Weinheim